Study of Active Faults: Theoretical and Applied Implications

V. G. Trifonov and A. I. Kozhurin

Geological Institute, Russian Academy of Sciences, Pyzhevskii per. 7, Moscow, 119017 Russia
e-mail: trifonov@ginras.ru
Received March 16, 2010

Abstract—Theoretical and applied implications of the study of active faults and their identification and parametrization are discussed. The term *active fault* is defined as a fault with displacements that occurred in the late Pleistocene and Holocene and are expected to resume in the future. The displaced young landforms, late Quaternary sediments, and man-made constructions are the main reference marks to recognize active faults and estimate their kinematics and intensity. Since the structural pattern and parameters of all active faults are referred to the same, geologically short time interval, they are important for the study of recent geodynamics and young tectogenesis on the global, regional, and local scales. The opportunities that are opened for such investigations are illustrated by verification of the real existence of the Okhotsk and Bering minor plates. With allowance for active faults, it is possible to make tectonic and geodynamic reconstructions of the past events more plausible. Natural hazards, primarily, earthquakes, are related to active faults. The geological and geomorphic assessment of the seismic potential of active fault zones is discussed with emphasis on the maximum possible magnitude of earthquakes (M_{max}) estimated from the segmentation of the active zones, the length of particular segments (L), the empirical relationships M_{max}/L for strong recent earthquakes, as well as the resumption periods of strong earthquakes and measurement of particular seismogenic offsets by trenching and other techniques, including archeoseismological methods. A question is posed about possible perennial variations in the stress-and-strain state of active zones, which are expressed on the scale of large seismoactive regions in oscillations of released seismic energy and should be taken into account by assessment of the seismic hazard.

DOI: 10.1134/S0016852110060051

INTRODUCTION

The terms *active fault* and *living fault* appeared in the American and European geological and seismological literatures in the late 1940s. The authors that introduced these terms [42, 68] used them for designation of faults accessible for geological observations and demonstrating contemporary movements, which anticipate similar movements in the near future. Later, the broader term *active tectonics* appeared by analogy with these terms [38].

The recent activity of faults attracted attention much earlier. Mushketov [15] argued for relationships of earthquakes with faults. Reactivation of faults was described in detail for the strong 1906 San Francisco earthquake in California [57] and the 1911 Kemin earthquake in the Tien Shan [2]. Since the mid-20th century, the interest in faults as sources of seismic and deformation impacts on buildings and other structures has increased dramatically, and active faults have become special objects of research.

As concerns the practical implications of active faults, two aspects should be distinguished. The first aspect is the use of active faults as seismogenerating zones for assessment of the seismic hazard of territories and objects. In addition to knowledge of fault geometry and the intensity and kinematics of displace-ments, another important element is the collection of data on the pulsed movements regarded as the causes of earthquakes and enabling estimation of their magnitude and age. The second aspect is the assessment of possible destruction and damage of engineering constructions affected by pulsed or continous faulting.

Furthermore, the study of active faults and related structure formation is important for understanding recent and contemporary tectogenesis. In combination with geophysical, petrological, and geochemical data on current processes at the deep levels of the geologic medium, active manifestations of tectogenesis at the Earth's surface make it possible to construct 3D models of the current evolution of the tectonosphere and to make tectonic and geodynamic reconstructions of past events more plausible.

The principles of the study and parametrization of active faults and their use for the assessment of seismic hazard are discussed in this paper along with some aspects of the recent geodynamics of mobile belts considered in the light of data on active faults.

CONCEPT OF ACTIVE FAULTS

Because movements along faults occur nonuniformly and often discretely (epochs or moments of displacements alternate with epochs of quiescence), it

is necessary to study a certain time interval close to the present moment, which is sufficient not only for documentation of fault activity but also for estimation of its parameters (sence, rate, regime of movements, etc.). In the opinion of Allen [39], such faults should be called active, which bears signs of Holocene (the last 10 000 years) movements. Nikonov [52] expanded this interval up to 400 000 years and thus involved the entire late and middle Neopleistocene. On the basis of research in the Alpine–Himalayan Belt and the western United States, Trifonov [30, 31] stated that the last 100–130 thousand years are necessary and sufficient to determine whether a fault is active and to assess its parameters and regime of development in the mobile belts.

It is implied that if during a certain time (10, 100–130, or 400 thousand years) at least one displacement along a fault has occurred, this gives grounds to expect with a certain assurance that the next displacement along this fault is possible in the near future. In fact, the selected time interval (see above) is accepted as the expected maximal recurrence interval of displacements along faults. If from the moment of the last displacement less time has elapsed than the period of resumption, it is reasonable to assume that the next displacement is probable in the near future and to classify the fault as active. If the duration of seismic silence of the fault since the last displacement exceeds the resumption period, the fault may be referred to as inactive.

The expectation of future displacement passes the fault into the category of active [68]. If there are no grounds for such an expectation, the fault should be classified as inactive. All other parameters, including the direction, average velocity of movement, etc., do not depend on the age of displacement and thus are not critical for understanding the term active fault. A fault can be active or inactive. Therefore, the classification of faults by degree of their activity is superfluous. Such classifications [11, 21] only reflect the degree of our knowledge of the fault.

The recurrence period in mobile belts and zones of continents established from the study of specific faults varies from a few hundred to a few thousand years [62] and may be even longer. For a fault in the East Kamchatka Zone, the age of the last displacement was determined at 9000 years [7]. The average recurrence period for the Umehara Fault in Japan was established by A. Okada at ~14 500 years [49]. It is evident that an average recurrence period is accepted for earthquakes. Recurrence periods measured in the hundreds of thousands of years remain unknown in the practice of special investigations. Taking into account the incomplete knowledge, it seems reasonable not to define exactly the duration of the critical interval of the maximum possible period of resumption and only to assume that it may reach a few tens of thousands of years.

IDENTIFICATION, STUDY, AND PARAMETRIZATION OF ACTIVE FAULTS

The period of a few ten thousand years from present day is the time during which the landforms commonly called young have been created. This implies that the main attribute of fault activity is the displacement of young, late Quaternary surfaces and any other landforms or sediments (see section "Paleoseismological Aspects"), as well as any artificial, e.g., archeological or historical objects (see section "Archeoseismological Aspects").

It is evident that the younger the most recent displacement, the more the surfaces are deformed and the more distinctly the fault is expressed in the topography. With increase in the resumption period, much older surfaces are affected by the last displacement and manifestations of faults move to the upper stages of the topography, i.e., to older surfaces. As a result, the fault line at the Earth's surface is dismembered into more fragments and becomes discontinuous and the fault scarp degrades and loses its steepness. In other words, the fault becomes poorly expressed in the topography. The random and insufficient character of the natural outcrops along its line makes identification of the fault and its classification as active still less reliable.

Various methods of studying active faults have repeatedly been discussed in the literature, although at first they were not called active [6, 8, 24, 25, 28, 30–32, 34, 37, 52, 63, 64].

Geological–Geomorphic Methods

The geological–geomorphic method is the main tool for studying active faults. Young sediments do not occur in all areas, and where they are present, outcrops are required. The irregular distribution and scarcity of natural outcrops is compensated by trenching, i.e., creation of artificial outcrops.

The kinematic analysis of displaced landforms is applicable almost everywhere and provides exact determination of the main parameters of active faults: the kinematics of movements (direction of displacements), their amplitude, the proportions of vertical and horizontal components, and the average velocities of movements when the displaced landforms can be dated. Radiocarbon dating is used most frequently; its time interval (up to ~50 000 years) covers the timespan necessary for the identification of active faults.

Despite the obvious similarity of all active faults, the interpretation of landforms whether they are controlled by or related to faulting is always specific. Several common rules of such interpretation are given below.

(1) It should verify that the formation of linear landforms, e.g., scarps of any surface, cannot be explained by the effect of nontectonic processes (erosion, denudation, accumulation, permafrost, etc.).
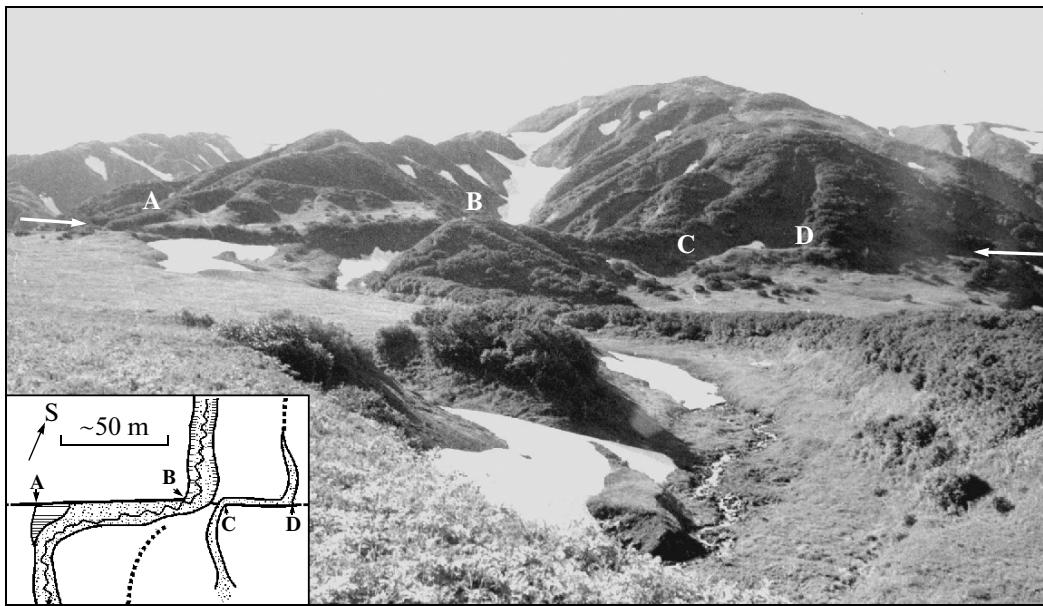
Fig. 1. Active right-lateral strike-slip fault, Kamchatsky Peninsula, Kamchatka, modified after [48]. The displacement in plan view is shown in the inset. Offset: A−B = 65−70 m; C−D = 30 m.

(2) The amount of accumulated fault deformation and the age of the displaced landforms should be coordinated.

(3) As a rule, the line of the inferred active fault should be mapable. In some cases, however, the lines of the proved active faults are drawn even in recently published geological maps on a scale of 1 : 200 000 as stratigraphic contacts.

(4) The inferred fault should be inscribed into the regional system of recent structural units as a natural element of the common structural grain.

The specific geomorphic manifestation of displacement in the topography is a combination of many factors, the most significant of which are the genetic type of the landform and the kinematic parameters of the fault. As a rule, an active fault is identified primarily as a scarp of a certain height, steepness, and morphology in cross section. It seems obvious that it would have to be this way in the case of vertical separation, however, strike-slip faults are also often traced as scarps. The displaced surfaces are never perfectly smooth and horizontal, so that the segments of the surface initially occurring at different heights can be juxtaposed at a certain point of the strike-slip fault. In this case, vertical separation is only apparent and does not indicate true vertical displacement.

Long-term motions (multiple displacements) along faults with predominant vertical component are expressed in abrupt variation in separation when passing from the surface of one age to the surface of another age or in cross section of the fault-line scarp. The strike-slip movements are best identified by offsets of water-stream valleys of various orders in plan view. The offset increases with the age of the stream or the element of its valley. Deviation of active channel is not obligatory; the relationship of the slip rate and lateral erosion in the displaced valley is the important factor in this respect. Embayed terraces and abandoned channels are typical results of strike-slip faulting (Fig. 1). In the latter case, the occurrence of an inactive depression connecting the abandoned and active channels along the fault is obligatory. The relationships between the components of motion along the faults are established most reliably from the displaced terraces of various, most often alluvial, origin. The vertical component is measured by the displacement of the terrace tread and the horizontal component by the offset of its riser.

The data from various regions show that movements along the same fault plane develop for a long time. In the considered example, the age of the movements, i.e., the displaced landforms, was limited by the Holocene or the end of the late Pleistocene. The Talas−Fergana Fault in the Tien Shan is a case when the movements along one fault plane are retained for a much longer time [66].

Paleoseismological Aspects

Trenching. The results of using trenching under diverse tectonic and landscape conditions are covered in many publications. Detailed descriptions of this technique can be found in two editions of *Paleoseismology* edited by J.P. McCalpin [53, 54] and in the book *The Geology of Earthquakes* by R.S. Yeats et al. [72]. The general principles of trenching [7] are briefly summarized below.

A trench is an artificial exposure that opens a fault at that fault-line point, which is most appropriate for estimation of the displacement frequency (recurrence), direction and amplitude of motion, and age of the last displacement. These data are called paleoseismological, or paleoseismogeological, because they allow judging about the approximate magnitude of the past strong earthquakes related to the given fault and to predict with a certain probability what one can expect from this fault in the future.

The interpretation of the faulted section is based on the traditional methods of structural analysis and analysis of the facies and thickness. The application of these methods to trenching requires taking into account that the movement along the fault deforms not only the rocks but also the ground surface, both on land and under the water. The deformation makes the ground surface uneven and leads to the deposition of sediments as products of leveling of surface irregularities by exogenic processes. Erosion, denudation, and accumulation, acting together for a certain time-span after displacement, form a new ground surface, which will be deformed by the next displacement, if it occurs. The restoration of the past ground surface (paleosurface) that existed up to the moment of displacement, the description of its deformation, and its dating are the basis of paleoseismological interpretation of the section. D. Pantosti et al. [55] called this surface the *event horizon*, which theoretically had zero age at the moment of displacement. Several such surfaces (event horizons) may be established in the given section, and each older surface is deformed by all subsequent events, i.e., displacements along the fault. Because of the specific structure of the particular section, the type of rocks, their lithological contrast, etc., some event horizons can remain unidentified and then an event is missed, or conversely, some elements of the section can be erroneously interpreted as indications of an irrelevant event, so that a superfluous event appears.

The study of a single trench, i.e., at a point on fault line, cannot characterize the fault as a whole, even if no events have been missed and no superfluous events have been added. While the direction of movement and average velocity of displacement over a relatively short period can be taken as representative for the entire fault, then the amplitude of single-shot displacement is an attribute pertaining only to the given point. To identify the pattern of changes in the amplitude of displacement along the fault's strike, a number of trenches should be dug up. The same may be said about the recurrence interval of displacements. Being determined for a particular fault, it cannot be extrapolated over the fault zone as a whole, and additional data must be obtained for each respective fault.

The sketch and interpretation of a trench crossing a fault in the East Kamchatka Zone [47] (Fig. 2) is given as an illustration of the aforesaid. This is a case with several displacements. The movement along the fault resulted in deformation of a postglacial terrace. The kinematics of displacement corresponds to a normal fault. The movement along the fault is expressed in deformation of the soil—pyroclastic cover and the boulder—pebble layer at its base. Five displacements are distinguished. The last two displacements took place 3200—3300 years ago. The ages of the three preceding displacements were determined at 10500, 6000, and 4500 years, respectively. The occurrence of two events close in age (3200—3300 years) is explained by the superposition of two seismic ruptures. If this was the case, then the average duration of the interval between displacements (resumption period) looks as follows: four displacements with the age of the oldest one at 10500 years and the age of the youngest at about 3000 years. They are separated by three time intervals, each about 2500 years in length. The later figure is the average resumption period, whereas particular intervals between displacements differ from one another: 3500, 1500, and 1200—1300 years.

As was mentioned above, a single trench is insufficient for characterization of the fault as a whole. Therefore, the average period of resumption should be regarded only as a probable estimate requiring confirmation.

Multiple strike-slip displacements along an active fault can be revealed from discrete horizontal offsets of landforms in a particular segment of the fault [30, 69]. The method is based on the suggestion that water streams crossing the fault are formed and evolve continuously. If continuous strike-slip movements occur, the histogram of the amplitude and number of displaced streams will include all amplitudes against the background of decrease in the large amplitudes accumulated over a long period of time. If movements along the fault occurred as strong seismic pulses separated by epochs of complete or relative tectonic quiescence, the histogram will demonstrate only some amplitudes corresponding to the displacements of one, two, three, etc., earthquakes, whereas the intermediate amplitudes will be reduced. Precisely this example is shown in Fig. 3, pertaining to the Hangay Fault in northern Mongolia [30]. The maximum displacement of 5—6 m characterizes the displacement during the 23.07.1905 Bolnay earthquake with magnitude $M_S > 8$. It is noteworthy that the maximums of larger amplitude, which are the combined displacements of several earthquakes, are estimated at 11 ± 1, 16.5 ± 1.5, 22 ± 0.5, 28.5 ± 1.5, 33 ± 1, 40 ± 1, and 45 ± 1 m, that is, divisible by the displacement of the Bolnay earthquake. These paleoearthquakes probably were close in magnitude. This method does not allow estimation of earthquake age. For the Hangay Fault, this problem has been settled by study of pits dug sunk in the shallow pull-apart basins or in the dammed deeps arising in curved segments of the strike-slip fault or its en-echelon arranged branches bounded by normal faults. Lacustrine and swamp facies mark the
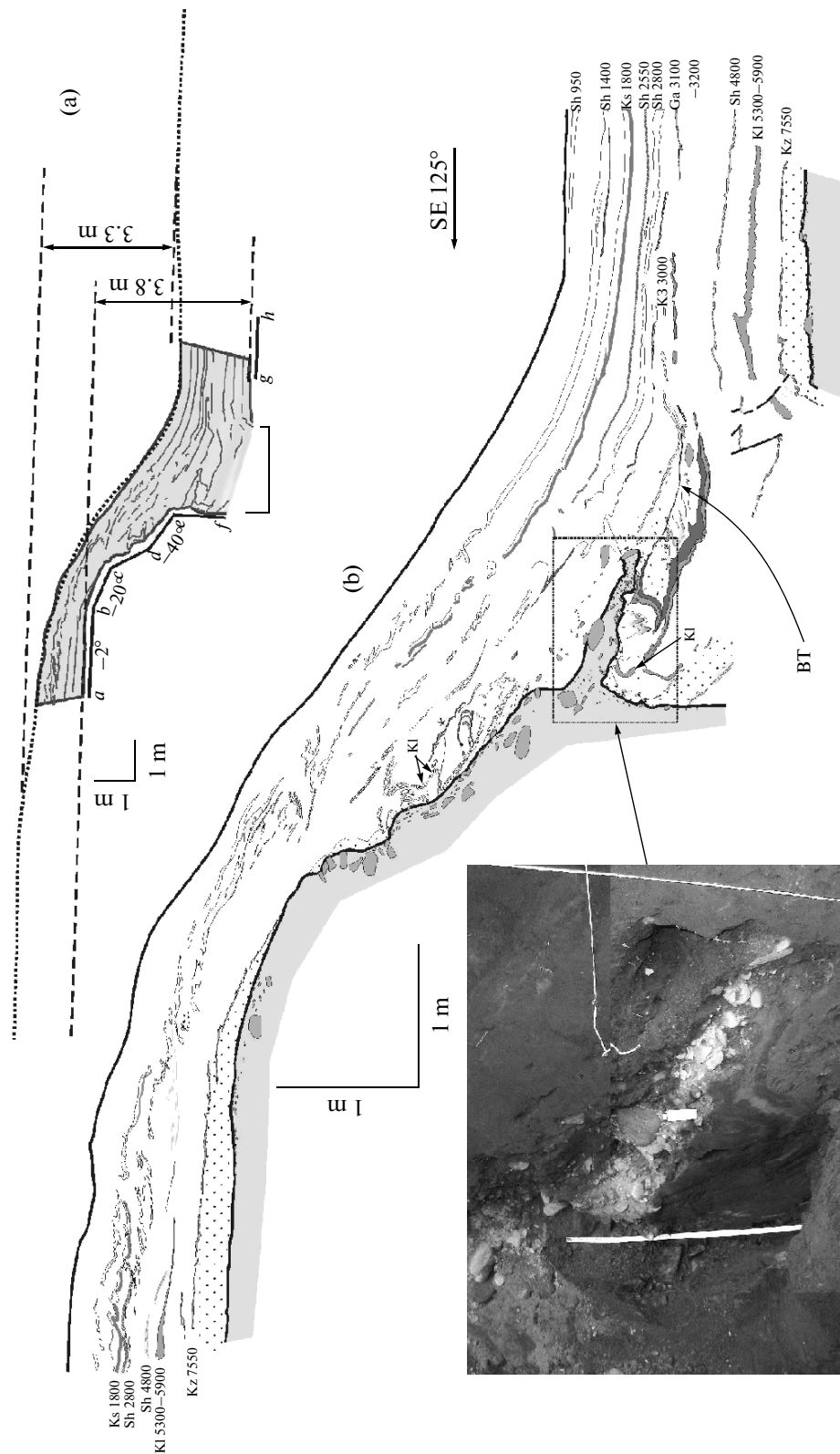
Fig. 2. Documentation and paleoseismological interpretation of the section exposed in trench, Kamchatka, after [48]: (a) parameters of trench and section: dotted line, terrace surface; dashed line, approximation of terrace surface and boulder–pebble layer; numbers in meters are amplitude of vertical separation of the boulder–pebble layer and ground surface; the bar below the base of the scarp indicates the fault-line depression; Roman letters and numerals (degree) indicate the end of fragments of the boulder–pebble layer and their slope; (b) sketch of the section (southwestern wall of the trench): gray, boulder–pebble layer at the base of soil–pyroclastic cover (separate boulders are shown); overlying tephra interbeds derived from Shiveluch (Sh), Ksudach (Ks), Gamchen (Ga), Klyuchevsky (Kl), and Kizimen (Kz) volcanoes; BT, thin interbed of black tephra; tephra interbeds are intercalated by soil units; numerals are radiocarbon age, years, B.C.; (c) interpetation of the section: numerals in circles are displacement from older to younger, in thousands of years: 1, 10.5; 2, 6.0; 3, 4.5; 4 and 5, 3.2–3.3; U2 and U3, unconformity surfaces (numerals correspond to displacement numbers); CW, colluvium wedge (numerals correspond to displacement numbers). Indications of displacement 1 are fragments of the slope of the degraded scarp of the boulder–pebble layer surface; WF and EF are the western and eastern fault planes, respectively.
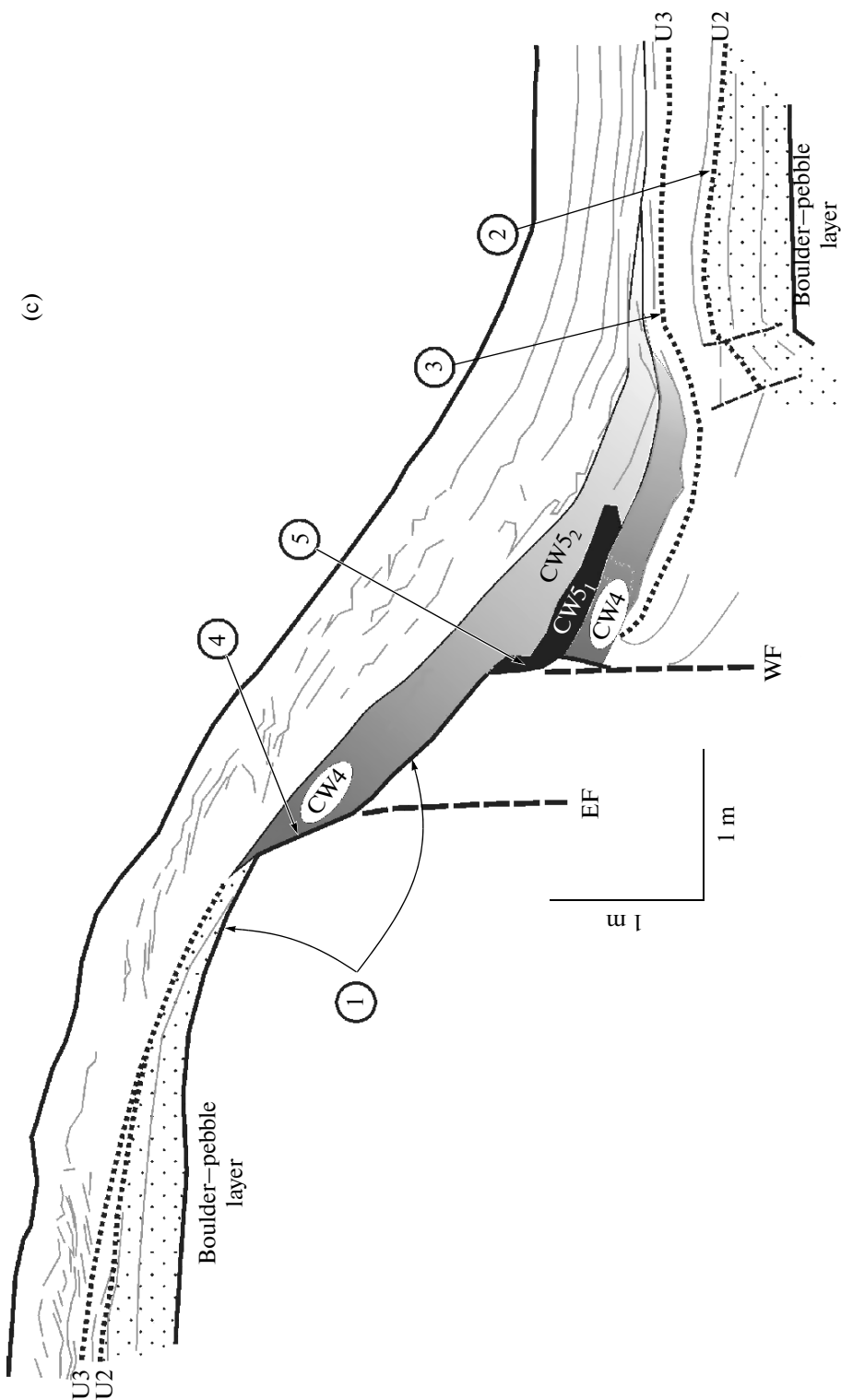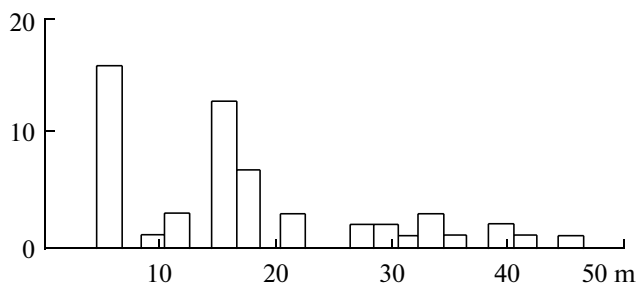
Fig. 2. (Contd.)

Fig. 3. Distribution of Late Holocene left-lateral offsets of small landforms along 15-km segment of the Hangay Fault at the northern slope of the Dagan-Del Range, northern Mongolia; *x*-axis, offset, m; *y*-axis, number of displaced landforms.

moments of basin deepening as a result of seismic displacement. Radiocarbon dating of these facies has made it possible to estimate the age of eight strong earthquakes over the last 4500 years [30]. Their resumption period was about 600 years.

Archeoseismological aspects

The occurrence of remnants of ancient constructions with distinct configuration is a precondition for the application of archeoseismological methods, which are especially efficient in the southern regions of Russia and the adjacent areas of the Transcaucasus region, Central Asia, China, and Mongolia. Three groups of problems are solved with the use of archeological data: (1) determination and specification of the parameters and seismic potential of active faults; (2) dating of displacement along faults and related structural elements; and (3) parametrization of preinstrumental earthquakes from characteristic damages.

Let us illustrate solutions of the problems pertaining to the first group by specific examples. The right-lateral strike-slip offset of an ancient grave by 4 m in the Mongolian Altay is shown in Fig. 4a. The grave is located on a young seismogenic fault, which coincides for ~160 km with the NW-trending active Kobdo (Khovt) Fault and in the south (~20 km) deviates from it to the south [30, 36]. Along the main 160-km segment, young streams are shifted 4−5 m to the right, and no offsets of smaller amplitudes are documented. In the south, the offset decreases. Thus, the offset of the grave and neighboring streams is a result of a single displacement during an earthquake whose magnitude is estimated from the M/L and M/D ratios (see below) at 7.7−8.0. Radiocarbon datings estimate the resumption period of such earthquakes in the fault zone at ~700−750 years and the average rate of slip at 5−6 mm/yr. This rate is close to the average rate of strike-slip displacement over the middle and late Neopleistocene (4−5 mm/yr) [30]. The grave is pre-Mongolian. Because catastrophic earthquakes in this region were not documented either in the epoch of Chingizides

(12th−14th centuries) or in the epoch of Chinese administration and later (since the late 17th century), it is most probable that the seismic event occurred in the 15th−16th centuries, which is in agreement with the radiocarbon dates.

Other examples demonstrate the cumulative effect of several earthquakes. The left-lateral offset of a Roman aqueduct along the main branch of the El-Gab Transform Fault of the Dead Sea near the village of Al Harif 5 km north of Mount Missiaf in western Syria was mentioned for the first time in [35]. The aqueduct was dated at the first century CE; the offset was estimated at 13.6 m and interpreted from the data of trenching as the cumulative effect of no less than three offsets, the last of which was probably related to the 1170 earthquake with $M_S = 7.7$ [51]. Later, the age of the aqueduct was specified (no older than 63 CE) [59]; the offset was specified as well [33]. The total offset is summed up of the slip of ~10 m along the main fault branch A−B and offsets along splays C−D by 1.0−1.5 m and E−F by 0.75 m (Figs. 4c−4e). The total offset of ~12 m over ~2000 years yields an average rate of slip of ~6 mm/yr.

Figure 4b shows the offset of an underground irrigative gallery along the Main Kopetdag right-lateral reverse−strike-slip fault near the settlement of Parou in Turkmenistan [31]. The gallery is manifested at the surface by a line of wells, called here kyarizes. This line is displaced along the fault by ~10 m. The remnants of abandoned wells indicate that the irrigative system was reconstructed twice after its damage. The damage was not a result of creep, because otherwise the system could not have functioned as long as it did. Obviously, the offset was pulsatory, i.e., seismogenic. After the last offset, the system was not rebuilt but superseded by a new one that is retained up to the present day. The first known description of kyarizes is referred to the fourth century B.C.; i.e., they appeared ~2500 years ago. If this line of kyarizes belongs to the oldest irrigative system and was damaged three times by earthquakes, the period of their resumption is ~800 years, and each offset was 3.0−3.5 m and thus corresponded to earthquakes with $M_S \sim 7.3$, similar to the magnitude of the 1947 Ashkhabad earthquake.

The left-lateral offset of an ancient wall [9] of a disrupted aqueduct [20] along the NE-trending Darwaz Fault in the Western Pamirs is interpreted in the same way as the cumulative effect of several seismogenic displacements (Fig. 4f). The wall was offset by 20−21 m during at least two epochs, first by ~15 m, and after rebuilding its extension was displaced by 5−6 m again. The aqueduct was related to mining of gold placers, and taking into account the regional history [32, 33], it may be suggested that the ~15-m offset was caused by seismic events in the third−tenth centuries CE and the second one by an event in the late 17th century.

The indications of seismogenic disruption recorded in damage to the Kal'at Sim'an monastery in
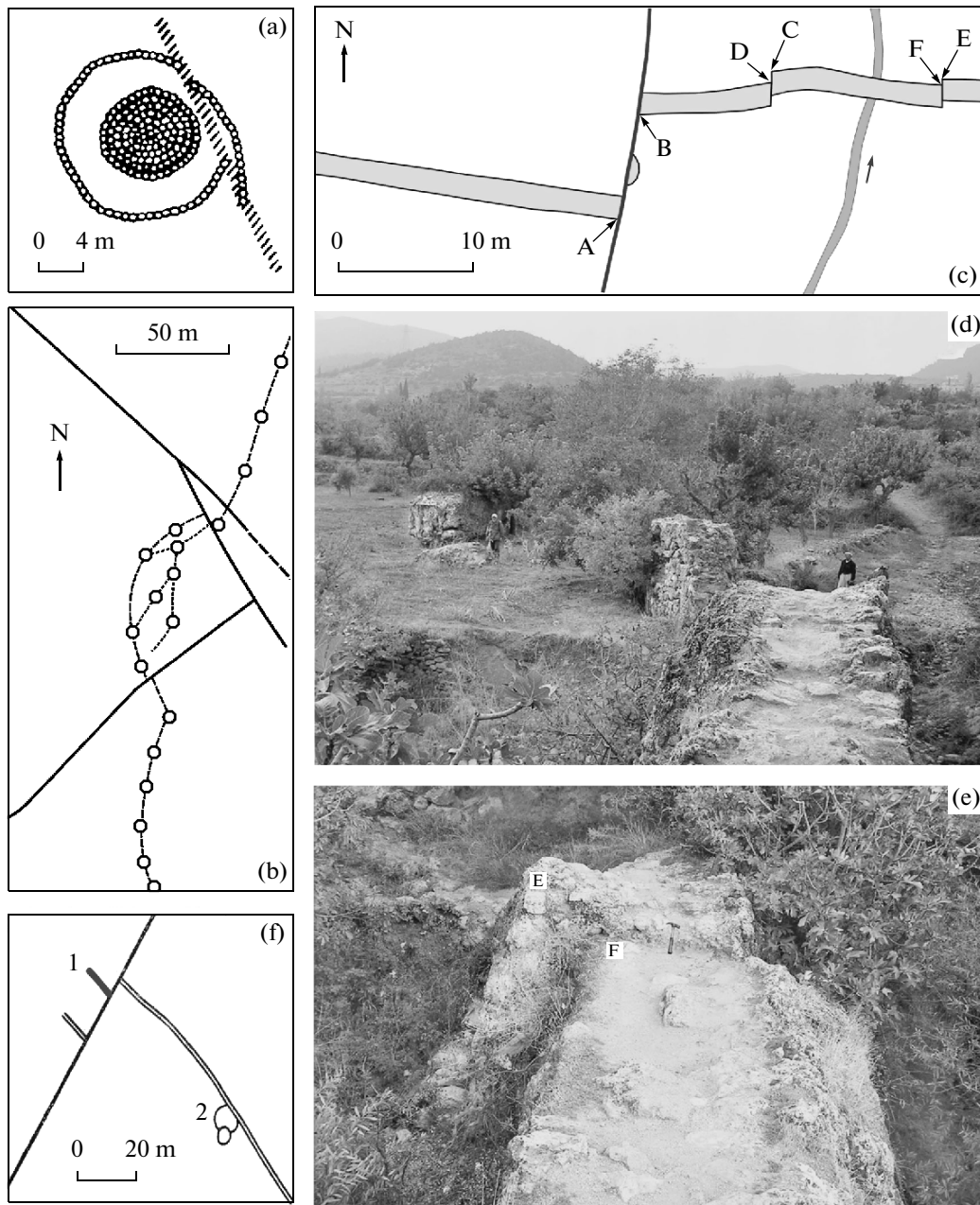
Fig. 4. Seismogenic displacements of archeological objects along active faults: (a) pre-Mongolian grave displaced along the right-lateral Kobdo (Khovd) Strike-Slip Fault to the south of the Ar-Khutel in the Mongolian Altay [30]; (b) underground irrigative gallery repeatedly displaced to the right along the Main Kopetdag Fault [31]; (c–e) aqueduct, first century B.C.–first century CE displaced to the left along the El-Gab segment of the Dead Sea Transform near Al Harif Village: (c) plan view of displacement, modified after [51], (d) displacement along faults A–B and C–D, (e) displacement along fault E–F; (f) Middle-Ages aqueduct displaced to the left along the Darwaz Fault 7 km southwest of Sagirdasht Village, Western Pamir (1, a new extension of the aqueduct built instead of the displaced segment; 2, later construction).

northwestern Syria have allowed estimation of the deformation of the interfault block [44]. The monastery is situated on the low-mountain Siman Range that extends in the NNE direction between two en-echelon arranged segments of the near-meridional left-lateral strike-slip fault zone. The extrusion of this range is caused by compression in the area of echeloned conjugation of the segments deviating by 10°

from the general trend of the strike-slip fault zone. The main temple of the monastery consists of a central octagonal atrium with remnants of the St. Simeon pillar in the middle and four crosswise adjoining three-nave basilicas. The northern and southern walls of the eastern basilica are curved relative to the rest of the construction by 6° (up to 2–3 m) to the north (counterclockwise) (Fig. 5a). The bases of older walls, addi-

tionally curved by 3° (up to 1 m), are retained nearby. Immediately to the west of the western extension of the temple, the base of the brickwork of an older entranceway is seen; afterward, the entranceway was shifted to the southern extension. The brickwork is curved relative to other elements of the construction by 9° (up to 3 m) clockwise. Finally, further to the west, in the zone of the western segment of the fault, remnants of the edifice are retained. Its southern wall is curved counterclockwise by dozens of centimeters, although this curvature could have been a defect of construction. All the aforementioned curvatures are not accompanied by visible fractures, i.e., are results of ductile deformation of the limestone basement and brickwork of the edifice. According to the model of lateral deformation of the main temple and the chapel that adjoins its eastern extension in the south, the rock massif of the Siman Range is squeezed to the south, where the distance between the en-echelon arranged fault segments increases (Fig. 5b). The counterclockwise bending of the edifice at the western margin of the monastery indicates a possible S-shaped lateral bending.

The deformations described above were the result of several strong earthquakes in the St. Simeon Fault Zone and in its immediate proximity. The main temple was built in 476−490 CE. The monastery was damaged seriously in the 528 earthquake ($M = 7.5$) but was restored by 560. The next events of seismic damage occurred in the 791, 951, and 972 ($M = 6.8$–6.9) earthquakes. The edifices were partly reconstructed in 976–986, when the monastery again fell under the rule of Byzantium. Subsequent damage and deformations were related to the seizure of the region by Arabs and Turks, as well as the strong 1407, 1626 and 1822 earthquakes.

The use of archeological data for solving the problems of the second group (dating of displaced objects) may be illustrated by an example that is related to the pre-Hellenic history of Troy, situated to the southwest of Dardanelles near the Aegean cost. The near-latitudinal Troy Fault with the uplifted southern wall extends between the Gessarlyk Ridge, where Troy was located, and the Dümrek (Simoeis, by Homer) Valley in the north [67]. The right-lateral offset is established in its segments oriented in the SSW−ENE direction [33]. In the west, where the fault reaches the Aegean Sea, a young terrace 1.5 m in height covered by fine-grained marine sand develops in both walls of the fault. Ceramic fragments from the time of Classical Greece were found on the terrace; the radiocarbon age of the soil (sample LU-5857) yielded 1545−1805 yr CE. The sand contains a layer of redeposited pumice, which is raised 0.4−0.5 m relative to the northern wall in the southern wall of the fault. The total right-lateral offset may have been greater.

The petrographic (M.I. Tuchkova) and chemical (S.M. Lyapunov) study of the pumice have shown its identity with the pumice of the Great Minoan erup-

tion on Santorini Island, which occurred in the late 17th or 16th century B.C. The former date fits better the ^{14}C determinations, whereas the latter is more consistent with the archeological data and seems to be more convincing [32]. As follows from the length of the Troy Fault (20−25 km) and the displacement of the pumice layer (>0.4−0.5 m), the earthquake magnitude which could be caused by this displacement [70] is estimated at $M = 6.7$. The earthquake took place after the Minoan eruption but before the time when sand emerged above sea level and transformed into the terrace with ceramic fragments. In the walls of Troy VI, signs of seismic impact are retained (Figs. 6e, 6f). This implies that the earthquake occurred either before or during the Trojan war, dated at ~1180 B.C.

To estimate the intensity of the tremor related to paleoearthquakes, it is important to solve problems of the third group focused on the study of the destruction and damage of archeological objects under the effect of secondary seismic disruptions and shock waves. Examples of such damage are described by Nikonov [1, 18] and systematized by Stiros [40]. The critical point is to distinguish seismic impacts from other disruptions and damages of ancient edifices (the results of decay, fire, war, etc.). We recognize three kinds of unambiguously seismic impacts on ancient edifices: (i) vertical or horizontal bending of walls often accompanied by rupture (Fig. 6); (ii) rotation of construction elements around the horizontal or vertical axes repeated in several neighboring edifices (Fig. 7); and (iii) fall of construction elements in one direction. The latter is exemplified in the eastward collapse of the wall of antique agora and columns in Palmyra, Syria (Fig. 8). Because the lower parts of the agora and most columns sanded-in to a height of 1−2 m in the Middle Ages did not undergo falling, the earthquake apparently occurred later. Sources report that a seismic event with epicenters to the northwest of Palmyra in the Palmyride Belt destroyed this town in 1089.

The above examples show that the results are most convincing when archeoseismological studies are combined with geological−geomorphic investigations of active faults, analysis of historical data, and paleoseismological evidence. In some cases, such a combination allows compilation of isoseist maps for preinstrumental earthquakes, which are important for parametrization of seismogenerating zones and estimation of their impact on the adjacent territories.

IMPLICATIONS OF THE STUDY OF ACTIVE FAULTS

Basic Scientific Implications of the Data on Active Faults

In general, faults are manifestations of brittle failure of the Earth's crust, and their clusters (zones) are considered to be expression of the divisibility of the Earth's crust and lithosphere into mobile and less
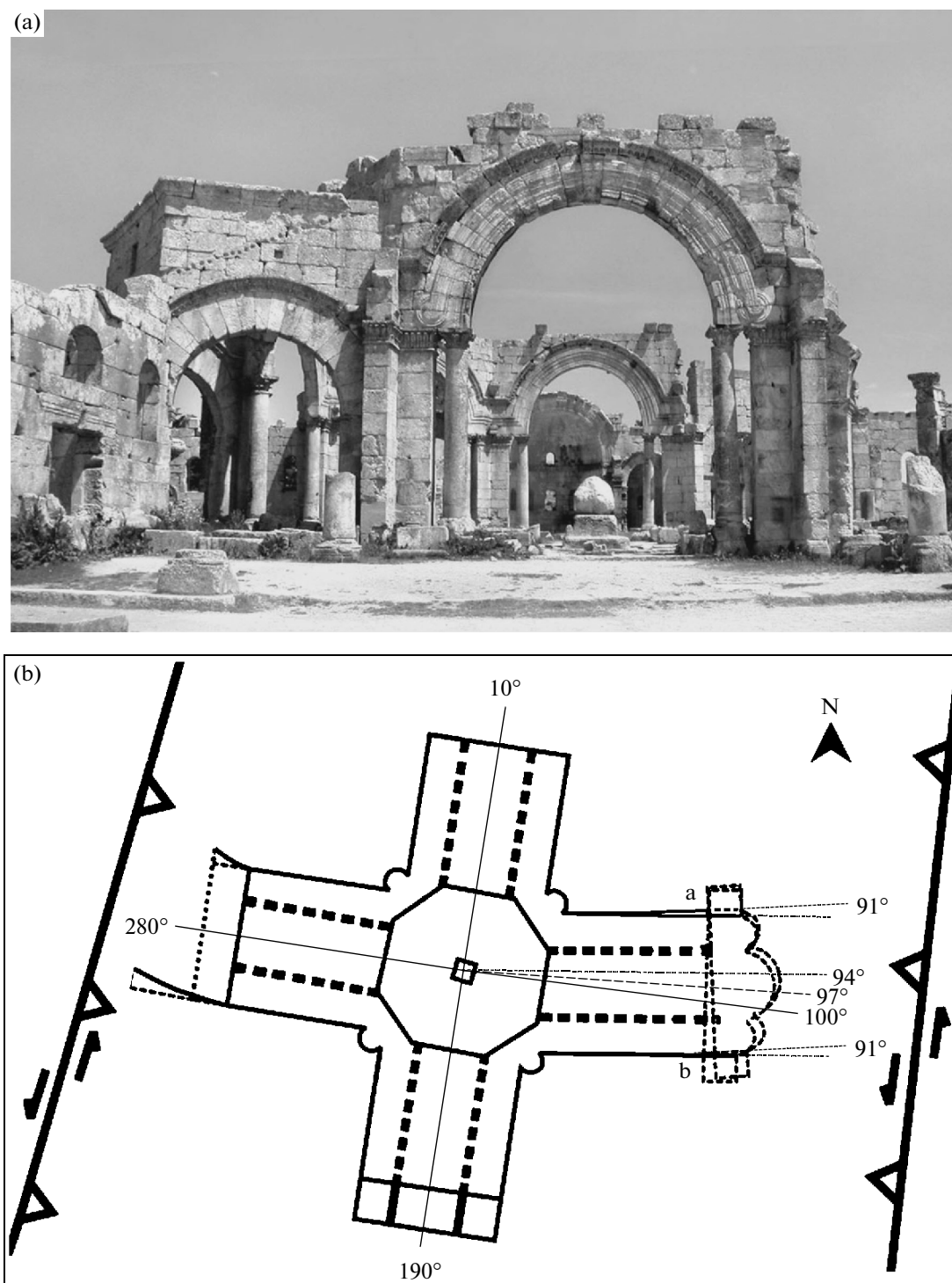
Fig. 5. Seismogenic deformation of the St. Simeon monastery in the zone of active left-lateral strike fault of the same name in Northwest Syria: (a) view on disrupted main temple from center of the western extension via central part to the eastern extension (along symmetry axis at an azimuth of 100° EES); the center of the sanctuary in the eastern extension deviates from this direction to the north; (b) model of seismic deformation of the main temple [44].
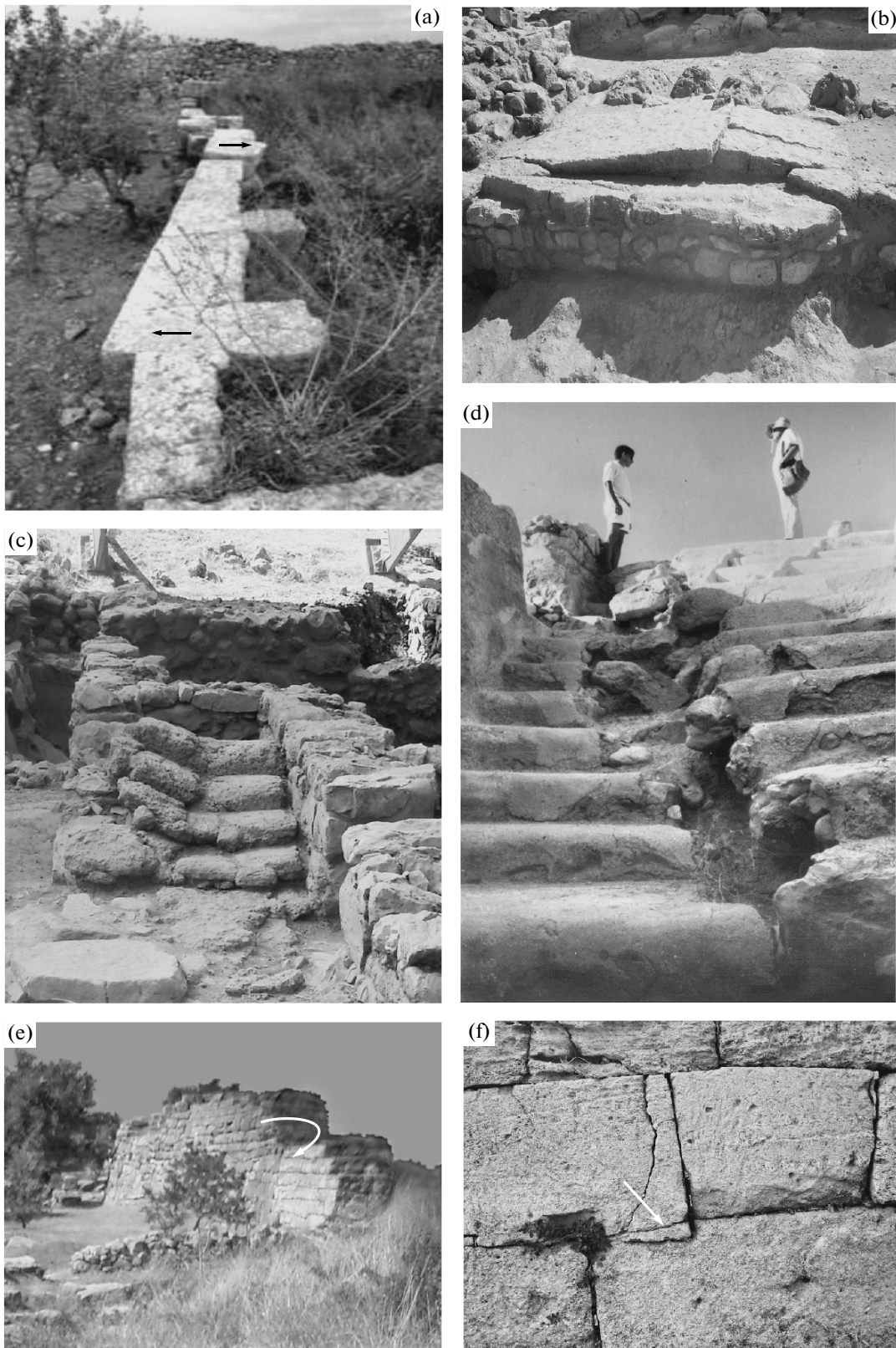
Fig. 6. Secondary seismic deformations and displacements of elements of ancient constructions: (a) Phoenician Ugarit, Late Bronze Age, West Syria, 1365 B.C. earthquake; (b) Knos palace, Late Bronze Age, Crete, Greece; (c) palace in Malia, Middle Bronze Age, Crete, Greece; (d) descent into pool, Khirbet–Qumran, first century B.C., Dead Sea, Israel, 31 B.C. earthquake; (e) Troy VI palace, Late Bronze Age, West Turkey, 1300 or 1180 B.C. earthquake; (f) fortress wall of Troy VI with damaged anti-seismic engagement.
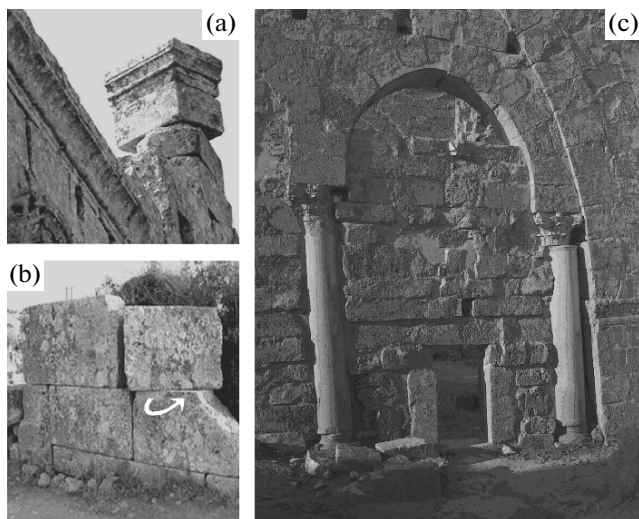
Fig. 7. Seismogenic rotation of blocks in ancient edifices: (a) baptisterium of St. Simeon monastery, late fifth–early sixth centuries CE, Northwest Syria, 528–529 earthquake; (b) Byzantian Thelanissos, fourth–sixth centuries CE, Northwest Syria; (c) Byzantian church in Rasafa, sixth century CE, right bank of Euphrates River, Syria.

Fig. 8. Unidirectional seismogenic fall of elements of ancient edifices of Palmyra, second–third centuries CE, Syria, resulting from 1089 earthquake: (a) fall of agora wall to the southeast; (b) rose diagram of column fall azimuths.

mobile belts along with relatively rigid, slightly deformed, or completely undeformed domains between them. The data on active faults fall on the same short time interval (late Pleisotocene and Holocene), and this makes it possible to consider even distant active structural elements as kinematically and dynamically linked, and thus, to restore the deformation regime of vast areas of the lithosphere, the crust, and the surface.

As an example of basic scientific application of the data on active faults, let us dwell on the demarcation of the Okhotsk and Bering lithospheric microplates in the northern framework of the Pacific on the basis of the assumption that the plate boundaries should be manifested in the system of active deformations and that such systems must be closed and continuous.

The boundaries of the Okhotsk Plate are commonly drawn along the deepwater trench of the Kuril–Kamchatka island arc, via Hokkaido Island, along Sakhalin Island, and further to the systems of uplifts of the Moma and Chersky Ranges in the north and then to the southeast toward the west end of the Aleutian island arc (Fig. 9). In the Sea of Okhotsk, the connecting link between the faults in Sakhalin and the northern Okhotsk region could be the meridional Kashevarovo Fault Zone [71] shifted to the east relative to Sakhalin.

Sakhalin is a tectonic rise, whose great extent from south to north is hardly accidental. It can be suggested that the system of active faults on this island are related to the formation and deformation of this rise and do not extend beyond its limits, in particular, beyond its northern end. None of the faults pertaining to the
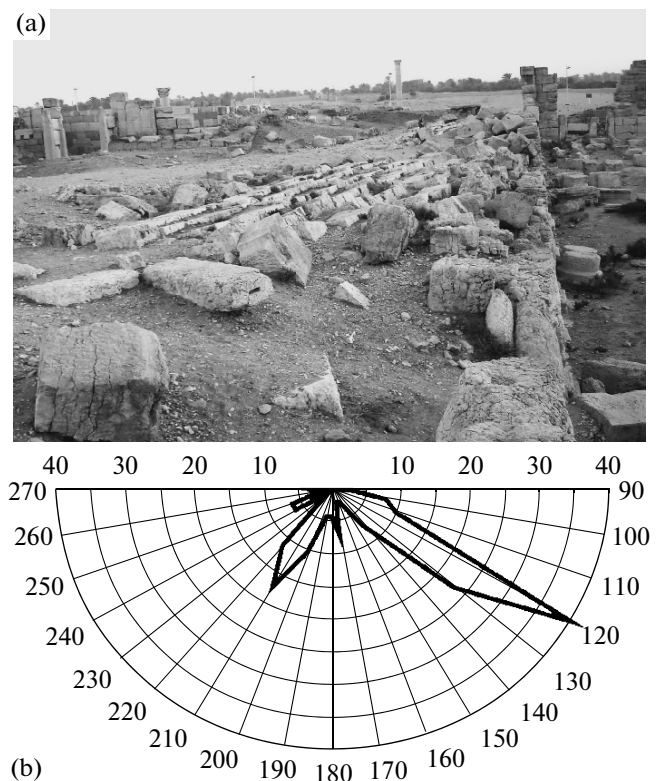
Kashevarovo Zone extend to the northern coast of the Sea of Okhotsk to join the single active Ketanda Fault. Although the distribution of recent instrumental seismicity is only an indirect rather than a decisive argument supporting the activity of a tectonic zone, it is nevertheless noteworthy that the Okhotsk Sea to the north of Sakhalin is completely aseismic.

It is suggested that the active Ulakhan Fault marks the boundary of the Okhotsk Plate in the North Okhotsk region and that the proved left-lateral movements along this fault and the inferred right-lateral movement along the Ketanda Fault provide the southward shift of the Okhotsk Plate relative to the Eurasian and North American plates [58]. The Ulakhan Fault, however, is traced to the southeast not further than to the southeastern margin of the Cenozoic Seimchan–Buyunda Basin; i.e., it ends approximately 150–160 km from the western coast of Shelikhov Bay. Over this 150-km tract, no NW-trending faults have been mapped. The most important argument to state that neither the Ulakhan Fault nor any other extend further to the southeast is the existence of the NE-trending Lankovo–Omolon Fault Zone that is traced along the northwestern coast of the Shelikhov Bay. This fault zone does not bear any sign of transverse ruptures, which can be expected if the NW-trending active faults
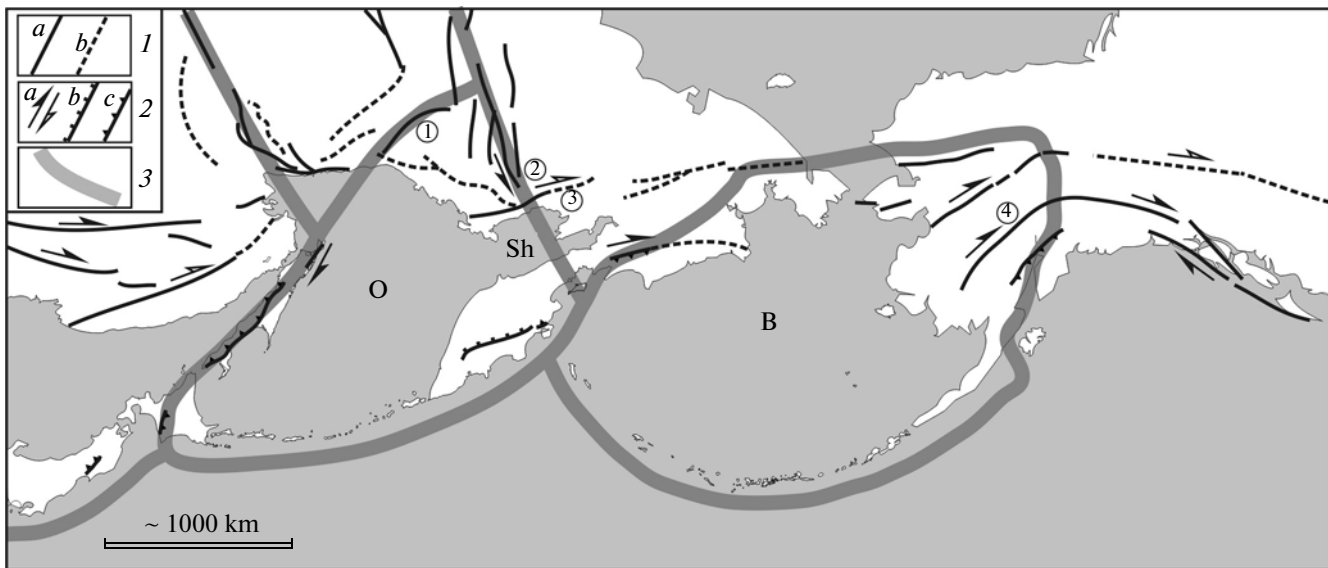
Fig. 9. Relationships between inferred boundaries of Okhotsk and Bering plates and main active faults. Solid gray lines are the boundaries of the Okhotsk (O) and Bering (B) plates, after [50, 58]; black lines are faults (dashed lines are inferred faults in Alaska, after [56], generalized); (*1*) active faults: (*a*) mapped and (*b*) inferred; (*2*) kinematics of faults: (*a*) strike-slip, open arrow for inferred displacement; (*b*) normal, and (*c*) reverse; (*3*) plate boundary. Faults and zones mentioned in the text (numerals in circles): 1, Ketanda; 2, Ulakahn; 3, Lankovo–Omolon; 4, Denali. Sh, Shelikhov Bay.

continue to Shelikhov Bay. On the other side of the Shelikhov Strait, in the western framework of the Komandorsky Deep, Quaternary or active transverse structural elements which can be interpreted as a manifestation of the northern boundary of the Okhotsk Plate are also unknown.

Thus, the boundaries of the plate reveal obvious gaps, and this implies that the principle of continuity of the plate boundaries is violated.

The Bering Plate in the configuration suggested in [50] also shows a lack of correspondence to the principle of reflection of plate boundaries in the linear zones of tectonic deformation. This is especially evident for the plate boundary in Alaska, where it is drawn from the Arctic coast to the Pacific Ocean across the right-lateral strike-slip faults of the peninsula. It turns out that the eastern latitudunal and NW-trending segments of the Denali Fault belong to the North American Plate, whereas the NE-trending southwestern segment, to the Bering Plate.

Thus, the data on active faults show that the issue of the existence of the Okhotsk and Bering microplates is far from indisputable. This compels us to consider alternative concepts concerning the tectonic processes in the northern framework of the Pacific, for example, the Sholl's extrusive model of active deformation in Alaska [60] or a model of a single transition zone with internal brittle–ductile deformations [46].

Assessment of Seismic Potential of Active Faults

The solution of problems concerning the seismic potential of a fault, i.e., the estimation of the maximum magnitudes (M_{max}) of earthquakes which could be induced by displacement along this fault, is based on the correlation between the parameters of the recent faults (lines of intersection of the fault plane with the ground surface along which displacement took place) and the characteristics of the induced earthquakes. The correlation links and the proposed regression equations rely on regional and global databases differing in volume and geographic coverage [4, 25, 27, 29, 61]. In general, the equations look as $M =$ a + b log$L$ and $M = c +$ d log$D$, where M is the magnitude, L is the length of the seismic fault, km, and D is the total displacement, m. According to the published data, coefficients a, b, c, and d vary widely in particular regions and over the globe as a whole. The relationships derived by Wells and Coppersmith [70] on the basis of the worldwide database are commonly used. These relationships connect the momentary magnitude of earthquakes, the length of the seismic fault, and single-shot displacements (maximal or average and with or without account of sence of displacement). Wells and Coppersmith have shown that the use of single-shot displacement (total, maximal, or average; with or without account of all components) as an independent variable results in widely scattered values. The main problem is that the value of single-shot displacement markedly varies along the faults, and no way is known to decide properly whether the ampli-

tude measured at one point is close to the maximum, minimum, or mean estimate. Some way out is possible only by identification of as many displacements as possible and by assessment of their variation along the fault.

The most probable maximum value (M_{max}) is determined when the length of the seismic fault is used as a variable. Consider arising problems.

It is known that large active fault zones generate earthquakes in separate segments (the superstrong 1960 Chilean or the 1964 Alaskan earthquakes that comprised several segments are the only exceptions, but they fall outside the scope of our discussion). Therefore, the segmentation of the active faults and fault zones is the most important factor in the estimation of M_{max} and calculation of M_{max}/L. The determination of the characteristic length of a fault, i.e., the length of that segment which can be renewed due to the future displacement (length of the future seismic rupture [41]), introduces much more uncertainty in the estimate of M_{max} than other parameters.

It is considered that fault segments differ in structural pattern and/or the main parameters of motion (velocity, direction, etc.) [72]. Such segments form separate echelons in the strike-slip fault zones, deviate from the general strike of the fault zone, and make up various conjugations. The segmentation of faults and fault zones is characterized by a certain probability, and no assurance can be achieved that the segment is chosen properly.

Note two examples of obvious discrepancy between contemporary seismic ruptures along the lines of active faults and their possible segmentation. The first example is a seismic rupture that arose during the 2002 earthquake ($M_w = 7.9$) related to the active Denali Fault in Alaska. This arcuate fault, latitudinal in its central part, gradually changes its strike to the northwestern in the east and conjugates there at an acute angle with the Totschunda Fault. It is evident that the junction of two faults should be regarded as one of the terminations of the future seismic rupture. At least, it could be suggested that the future seismic rupture will extend by a certain distance along the Denali Fault, retaining its strike. Actually, the 2002 earthquake followed the least probable scenario. The seismic rupture extended along the Denali Fault eastward from the epicenter and then turned and extended for 70 km along the Totschunda Fault [43].

The second example is the seismic rupture of the 2006 Olyutor earthquake ($M_w = 7.6$). This seismic rupture is made up of several echelons about 140 km in total length [22, 23]. The central and northeastern echelons differ in kinematics (right-lateral strike-slip and reverse, respectively). It is commonly accepted that a gap of hundreds of meters between echelons cannot be a termination of a fault segment [72]. In this case, the gap is 14 km. In other words, before the earthquake the two en-echelon arranged segments of the active fault most likely would have been regarded as different segments.

Despite the aforementioned complications, the considered approach to determination of M_{max} of a future earthquake remains the only one that is accessible and used in practice. With some variations, it has been used for compilation of maps of general seismic demarcation (GSD-97) and will be used in GSD-2012. The progress in this regard will be achieved largely by expansion of the databases and related specification of the relationships between the parameters of displacements along the faults and the induced earthquakes. The segmentation of active faults will apparently remain an unsolved problem.

Variation of the Rate of Elastic Deformation Accumulation in Fault Zones

All maps of general and local seismic demarcation in Russia and abroad are based on a common principle: if an earthquake of a certain maximal magnitude has been recorded in the active seismic zone with instrumental, historical, or archeo- or paleoseismological methods, then the maximum magnitude of earthquakes expected in the future is taken as not lower than that of the recorded event (with different probability for different time spans). The relationships between the earthquake magnitudes and resumption periods are assumed to be constant over the entire time interval accounted for in the calculations (up to ten thousand years). This approach ignores probable variations in the stress-and-strain state. The data presented below indicate that such variations are possible, though they remain conjectural.

The cyclicity of seismic events in the best-studied active fault zones was established in the Alpine–Himalayan Belt between 15 and 80°E from the data on instrumental and historical earthquakes supplemented by archeo- or paleoseismological data. These cycles vary in duration from 300 to 700–800 years and occasionally longer; they do not coincide in time. The temporal distribution of seismic energy released in the belt over 5000 years was calculated on the basis of a corrected catalogue of strong ($M_S > 5.7$) earthquakes [32]. Although the catalogues comprise only strong events, the used catalogue turned out to be incomplete, and the presented histogram primarily reflects only a gradual decrease of our knowledge back to the past (Fig. 10a). Nevertheless, long-term variations are outlined.

To overcome the effect of diminishing knowledge and reveal the outlined variations in seismicity, we used the catalogue with two corrections. First, taking into account an approximate estimate of the number of unrecorded preinstrumental seismic events [5], we increased by 1.5 times the amount of seismic energy released by earthquakes in the 18th and 19th centuries and by two times the energy of earlier seismic events in comparison with instrumental earthquakes recorded
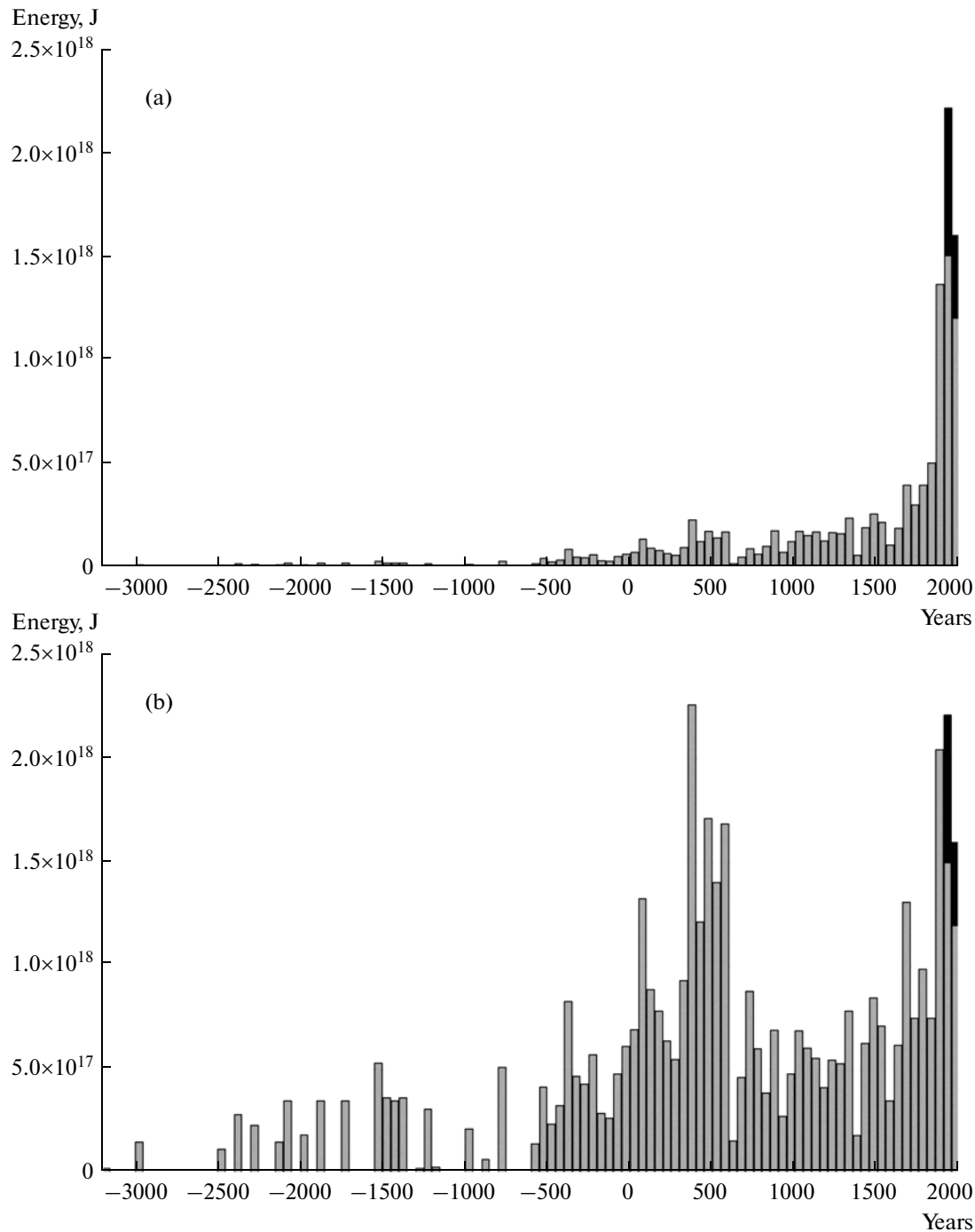
Fig. 10. Seismic energy, J, released by earthquakes with $M_S \geq 5.7$ in the central part of the Alpine–Himalayan Mountain Belt from the Carpathian–Balkan and Aegean regions to Central Asia from 3200 B.C. to the end of the 20th century CE: (a) modified after [32] and (b) the same histogram corrected for incomplete recording of strong preinstrumental earthquakes and area of their stable recording. Histograms were plotted by 50-year time intervals. Energy released by intermediate earthquakes (sources deeper than 70 km) is shown by black color.

in the 20th century. Second, historical earthquakes were normalized with allowance for areas of their stable records.

The ancient seismic events were revealed over small areas with archeo- and paleoseismological methods. From the middle of the first millennium B.C. to the

second half of the first millennium CE, the regions of stable recording were limited to the Mediterranean and Near East. In the 9th–10th centuries, with the flowering of the Arabian Halifat, this area expanded to the Middle East and oases of Central Asia, and in the 12th century expanded to cover Southeast Europe. In

India and the mountains of Central Asia, strong earthquakes began to be recorded only in the 19th century with the arrival of the English and Russian colonial administrations. After the introduction of corrections into the histogram of released seismic energy, the general cyclicity of seismic events is shown more distinctly (Fig. 10b). In addition to a two-humped outburst of seismicity from the mid-17th to mid-20th centuries, the same outburst was outlined from the mid-fourth to the late sixth centuries. The outburst of the 15th—13th centuries B.C., which was established from archeo- and paleoseismological data, is made up of the strongest earthquakes related to the Great Minoan eruption of Santorini, but their nature is clearly distinct. Finally, a vague maximum is outlined from the 25th to the first half of the 23rd century B.C. The time intervals with comparable phases of outbursts are different: 1250—1300 years between the first and second, 1800—1850 years between the second and third, and 1300—1350 years between the third and fourth phases.

It was suggested that the cyclicity and synchronous climatic changes were controlled by variations in the rotation of the geospheres manifested in variations of the magnetic field [3, 32]. In any case, they differ from common seismic cycles and probably reflect fluctuations in the stress-and-strain state of the active zones. Regardless of the nature of such fluctuations, the probability of earthquakes with maximal magnitude in the early 21st century became lower than in the late 19th—early 20th centuries. This aspect of variation in seismicity requires further study.

Active Tectonics of Platforms

To date, no faults reliably displacing late Quaternary sediments or landforms have been documented in the East European Platform, especially as concerns its central areas distant from the adjacent mobile belts. Two explanations may be proposed to explain this feature.

(1) The probability of revealing active faults is low, considering the extremely low rate of accumulation of elastic deformation at the accepted resumption period (400 000 years) [52] (recall that such a duration of the resumption period is unknown in the practice of special investigations). For example, a single-shot displacement by 1 m corresponds to the average rate of displacement along the fault of only 0.0025 mm per year. In addition, it must be kept in mind that the topography of the largest part of the platform is markedly modified by Quaternary glacial processes, so that older surfaces are retained only fragmentarily in uplifted areas. The probability of Holocene displacements at the adopted maximal resumption period (400 000 years) is negligibly low.

(2) The second explanation assumes that faulting in the platform is a low-probability process in principle. This follows from the extremely low gradients of recent and contemporary movements corresponding to insignificant slopes (fractions of degree) of the main interfaces in the Earth's crust, beds of sedimentary cover, and topography [12].

It can be suggested that faulting is more probable in marginal parts of the platform close to its mobile framework. Fault planes displacing young loose sediments (including upper Holocene beds a few thousand years in age) were observed by Nikonov [19] in some localities within a wide transitional zone between the Russian Plate and the Fennoscandian Shield. Nikolaeva [16] reported postglacial seismodeformations, including primary seismotectonic and normal-fault scarps up to 20—25 m high, in the north of the Kola Peninsula. For all the importance of these observations, it should be said, however, that their tectonic interpretation requires additional substantiation. For example, Levkov [10] referred low-amplitude faults in the fine-grained fluvioglacial sediments to near-surface glaciotectonic phenomena; the parameters of the inferred faults in the Kola Peninsula (height of scarps and width of deformation zone disproportionate to short length) differ from the typical faults in the mobile belts. Nonetheless, linear elements in the present-day appearance of platform actually exist and can be defined as lineaments diverse in origin, requiring special study for each particular case. The general solution was proposed by Makarov [14], who substantiated the young (Quaternary) age of such lineaments and defined them as geodynamically active zones in the platforms—linear and occasionally isometric bodies of the Earth's crust with elevated gradients of stress, strain, and movement.

CONCLUSIONS

The theoretical and applied implications of active faults and methods of their identification and parametrization are discussed in this paper. A number of natural hazards are related to active faults. In addition to surface deformation, earthquakes, and volcanic eruptions, these hazards include collapses and landslides (not always seismogenic); sinks of various origins; permafrost and thermokarst phenomena; hydrogeological fluctuations; anomalous occurrences of erosion, abrasion, and accumulatiion; and pathogenic and even mutagenic effects on biota and mankind. Their effect can be increased by the influence of technogenic factors (mining, pumping-out of water and hydrocarbons, filling of water reservoirs, laying of communications, change of vegetation, etc.). Diverse natural processes and technogenic impacts on them interact, and their combined effect on engineering constructions may become catastrophic, even when the impact of each process taken individually does not reach the catastrophic threshold.

REFERENCES

1. I. A. Antonova and A. A. Nikonov, "Traces of Catastrophic Earthquakes in Hersones and Its Outskirts in the Roman Time and the Early Middle Ages," in *Essays of History of the Christian Hersones* (Aleteiya, St. Petersburg, 2009), pp. 14−51 [in Russian].

2. K. I. Bogdanovich, I. M. Kark, V. Ya. Korol'kov, and D. I. Mushketov, "Earthquake in the Northern Chains of the Tien Shan of the 22nd December 1910 (4th January 1911)," Trudy Geol. Kom., Nov, Ser. **89**, 1−170 (1914).

3. S. P. Burlatskaya, *Archeomagnetism: Study of Older Magnetic Field* (IFZ AN SSSR, Moscow, 1987) [in Russian].

4. A. V. Vakov, "Geometric Parameters of Sources and Magnitudes of Earthquakes with Various Types of Movements," Voprosy Inzhenernoi Seismologii, No. 33, 40−53 (1992).

5. G. L. Golinsky, Candidate's Dissertation In Physics and Mathematics (Moscow, 2000).

6. A. I. Kozhurin and G. A. Vostrikov, "Near-Oceanic Mobile Belts," in *Neotectonics and Contemporary Geodynamics of Mobile Belts* (Nauka, Moscow, 1988), pp. 67−151 [in Russian].

7. A. I. Kozhurin, V. V. Ponomareva, and T. K. Pinegina, "Active Fault Tectonics in the South of Central Kamchatka," Vestnik KRAUNTs, Ser. Nauki o Zemle **2** (12), 7−24 (2008).

8. M. L. Kopp, L. M. Rastsvetaev, and V. G. Trifonov, "Tectonic Fractures Formed at Holocene Earthquakes in the Central Kopetdag and Its Foothills," Izv. Akad. Nauk SSSR, Ser. Geol., No. 7, 59−69 (1964).

9. V. K. Kuchai and V. G. Trifonov, "Young Left-Lateral Strike-Slip Fault in the Darwaz−Karakul Fault," Geotektonika **11** (3), 91−105 (1977).

10. E. A. Levkov, *Glaciotectonics* (Nauka i Tekhnika: Minsk, 1980) [in Russian].

11. O. V. Lunina, "Formalized Estimation of Fault Activity in Pliocene and Quaternary: A Case of Baikal Rift Zone," Geol. Geofiz. **51**, 2010 (in press).

12. V. I. Makarov, "Some Problems in the Study of Neotectonics in Platform Territories: The Case of Russian Plate," Razved. Okhr. Nedr, No. 1, 20−26 (1997).

13. V. I. Makarov, "Quaternary Tectonics and Geodynamics of Platform Territories: Topical Problems," Byull. Kom. Izuch. Chetvertichnogo Perioda, No. 68, 10−25 (2008).

14. V. I. Makarov, A. L. Dorozhko, N. V. Makarova, and V. M. Makeev, "Contemporary Geodynamically Active Zones of Platforms," Geoekologiya, No. 2, 99−110 (2007).

15. I. V. Mushketov, "The Verny Earthquake of the 28 May (9 June) 1887," Tr. Geolkoma **10** (1), 1−154 (1890).

16. S. B. Nikolaeva, "Disastrous Earthquakes in the Vicinities of the Town of Murmansk: Paleoseismological and Geological Evidence," Vulkanol. Seismol., No. 3, 52−61 (2008) [J. Volcanol. Seismol. **2** (3), 169−198 (2008)].

17. A. A. Nikonov, *Holocene and Contemporary Movements of the Earth's Crust: Geology, Geomorphology, and Seismotectonics* (Nauka, Moscow, 1977) [in Russian].

18. A. A. Nikonov, "Collapse of Antique Dioscuria and Sebastopolis as a Result of Seismic Impacts," Geoekologiya, No. 4, 104−115 (1997).

19. A. A. Nikonov, "Main Features of Neotectonics and Geodynamics of the Transitional Tract from the Fennoscandian Shield to the Russian Plate," in *Proceedings of the 43rd Tectonic Conference on the Tectonic and Geodynamics of Phanerozoic Foldbelts and Platforms* (GEOS, Moscow, 2010), Vol. 2, pp. 97−100 [in Russian].

20. A. A. Nikonov, I. A. Veselov, and A. V. Vakov, "Deformation of Ancient Irrigative Channels As Indicators of Seismotectonic Movements along Large Fault Zones at the Northern Flank of the Pamir," in *Forecasting of Large Seismic Impacts* (Moscow, 1984), pp. 137−147 [in Russian].

21. N. I. Ovsyuchenko, "Study of Recent Seismic Activity in Regions of Seismic Hazard," Geoprofi, No. 1, 51−55 (2006).

22. T. K. Pinegina and T. G. Konstantinova, "Macroseismic Inspection of Consequences of the April 21, 2006 Olyutor Earthquake," Vestnik KRAUNTs, Ser. Nauki o Zemle, No. 7, 169−173 (2006).

23. E. A. Rogozhin, A. N. Ovsyuchenko, A. V. Marakhanov, and S. S. Novikov, "Tectonic Position and Geological Manifestations of the 2006 Olyutor Earthquake in Koryakia," Geotektonika **43** (6), 3−23 (2009) [Geotectonics **43** (6), 443−461 (2009)].

24. V. P. Solonenko, "Paleoseismogeology," Izv. Akad. Nauk SSSR, Fiz. Zem., No. 9, 3−16 (1973).

25. V. P. Solonenko, A. L. Treskov, V. M. Zhilkin, et al., *Seismotectonics and Seismicity of the Baikal Rift System* (Nauka, Moscow, 1968) [in Russian].

26. A. L. Strom, "Comparison of Parameters of Recent and Paleoseismic Dislocations," Fiz. Zemli, **29** (9), 38−42 (1993).

27. A. L. Strom and A. A. Nikonov, "Relations between the Seismogenic Fault Parameters and Earthquake Magnitude," Fiz. Zemli **33** (12), 55−67 (1997) [Izv. Physics Solid Earth **33** (12), 1011−1022].

28. V. G. Trifonov, "Aerospace and Ground Methods of the Study of Young Faults: A Case of Kopetdag," in *Study of Natural Medium by Aerospace Methods. Geology and Geomorphology.* (VINITI, Moscow, 1976), Vol. 5, pp. 103−113 [in Russian].

29. V. G. Trifonov, *Late Quaternary Tectogenesis* (Nauka, Moscow, 1983) [in Russian].

30. V. G. Trifonov, "Development of Active Faults," Geotektonika **19** (2), 16−26 (1985).

31. V. G. Trifonov, "Common and Specific Contemporary Geodynamics of Continents," in *Geodynamics and Evolution of the Tectonosphere* (Nauka, Moscow, 1991), pp. 144−160 [in Russian].

32. V. G. Trifonov and A. S. Karakhanyan, *Geodynamics and History of Civilization* (Nauka, Moscow, 2004) [in Russian].

33. V. G. Trifonov and A. S. Karakhanyan, *Dynamics of the Earth and Evolution of Human Society* (OGI, Moscow, 2008) [in Russian].

34. V. G. Trifonov, O. V. Soboleva, R. V. Trifonov, and G. A. Vostrikov, *Contemporary Geodynamics of the Alpine−Himalayan Collision Belt* (GEOS, Moscow, 2002) [in Russian].

35. V. G. Trifonov, V. M. Trubikhin, Zh. Adzhamyan, et al., "The Levant Fault Zone in Northwestern Syria," Geotektonika **25** (2), 63−75 (1991).

36. S. D. Khil'ko, R. A. Kurushin, V. M. Kochetkov, et al., *Earthquakes and Principles of Seismic Demarcation of Mongolia* (Nauka, Moscow, 1985) [in Russian].

37. V. S. Khromovskikh, *Seismogeology of Southern Baikal Region* (Nauka, Moscow, 1965) [in Russian].

38. *Active Tectonics* (Nat. Acad. Press, Washington, DC, 1986).

39. C. R. Allen, "Geological Criteria for Evaluating Seismicity," Geo-Mar. Lett. **86** (8), 1041−1057 (1975).

40. *Archaeoseismololy*, Ed. by S. Stiros and R. E. Jones (I.G.M.E. and the British School at Athens, Fitch Lab. Occasional paper 7. Oxford: Oxbow Books, Athens, 1996).

41. C. M. DePolo, D. G. Clark, D. B. Slemmons, and A. R. Ramelli, "Historical Surface Faulting in the Basin and Range Province, Western North America: Implications for Fault Segmentation," J. Struct. Geol. **13** (2), 123−136 (1991).

42. Geologische Rdsch. **43** 1955.

43. P. J. Haeussler, D. P. Schwartz, T. E. Dawson, et al., "Surface Rupture and Slip Distribution of the Denali and Totschunda Faults in the 3 November 2002 M 7.9 Earthquake, Alaska," Bull. Seismol. Soc. Amer. **94** (6B), 23−52 (2004).

44. A. S. Karakhanian, V. G. Trifonov, T. P. Ivanova, et al., "Seismic Deformation in the St. Simeon Monasteries (Qal'at Sim'an), Northwestern Syria," Tectonophysics **453**, 122−147 (2008).

45. M. O. Korfmann, *Troia/Wilusa. Guidebook* (Canakkale-Tübingen Troia Foundation, Tübingen, 2005).

46. A. I. Kozhurin, "Active Faulting at the Eurasian, North American, and Pacific Plates Junction," Tectonophysics **380**, 273−285 (2004).

47. A. I. Kozhurin, V. Acocella, P. R. Kyle, et al., "Trenching Active Faults in Kamchatka, Russia: Paleoseismological and Tectonic Implications," Tectonophysics **417**, 285−304 (2006).

48. A. I. Kozhurin, "Active Faulting in the Kamchatsky Peninsula, Kamchatka-Aleutian Junction," in *Volcanism and Subduction: The Kamchatka Region* (AGU, Geophysical Monograph Series), Vol. 172, pp. 111−120.

49. T. Kumamoto, "Long-Term Conditional Seismic Hazard of Quaternary Active Faults in Japan," J. Seismol. Soc. Japan **50**, 53−71 (1998).

50. K. G. Mackey, K. Fujita, L. V. Gunbina, et al., "Seismicity of the Bering Strait Region: Evidence for a Bering Block," Geology **25**, 979−982 (1997).

51. M. Meghraoui, F. Gomez, R. Sbeinati, et al., "Evidence for 830 Years of Seismic Quiescence from Palaeoseismology, Archaeoseismology and Historical Seismicity along the Dead Sea Fault in Syria," Earth Planet. Sci. Lett. **210**, 35−52 (2003).

52. A. A. Nikonov, "Active Faults: Definition and Identification Problems," in *Research on Active Faults* (Seismol. Press, Beijing, 1995), pp. 140−152.

53. *Paleoseismology,* Ed. by J.P. McCalpin (Intern. Geophys. Series, Academic Press, 1996), Vol. 62.

54. *Paleoseismology*, Ed. by J.P. McCalpin, 2nd Ed. (Intern. Geophys. Series, Vol. 95. Academic Press, 1996), Vol. 95.

55. D. Pantosti, D. P. Schwartz, and G. Valensise, "Paleoseismology along the 1980 Surface Rupture of the Irpinia Fault: Implications for Earthquake Recurrence in the Southern Apennines, Italy," J. Geophys. Res. **98**, 6561−6577 (1993).

56. G. Plafker and H. C. Berg, "Overview of the Geology ang Tectonic Evolution of Alaska," in *The Geology of North America, Vol. G-1: The Geology of Alaska*, Ed. by G. Plafker and H. C. Berg (Geol. Soc. America, Boulder, 1994), pp. 989−1022.

57. H. F. Reid, *The California Earthquake of April 18, 2006* (Carnegie Inst. Publ., Washington, 1910), Vol. 2.

58. S. A. Riegel, K. Fujita, B. M. Koz'min, et al., "Extrusion Tectonics of the Okhotsk Plate, Northeast Asia," Geophys. Rev. Lett. **20**, 607−610 (1993).

59. M. R. Sbeinati, M. Meghraoui, G. Suleyman, et al., "Timing of Earthquake Ruptures at the Al Harif Aqueduct (Dead Sea Fault) from Archaeoseismology, Paleoseismology and Tufa Cores," in *Abstracts of Intern. Workshop on Active Tectonic Studies and Earthquake Hazard Assessment in Syria* (Damascus, 2009), p. 78.

60. D. W. Scholl, "Viewing the Tectonic Evolution of the Kamchatka−Aleutian (Kat) Connection with an Alaska Crustal Extrusion Perspective," in *Volcanism and Subduction: The Kamchatka Region* (AGU, Geophysical Monograph Series), Vol. 172, pp. 3−36.

61. N. V. Shebalin, V. G. Trifonov, A. I. Kozhurin, et al., "A Unified Seismotectonic Zonation of Northern Eurasia," J. Earthquake Predict. Res. **8** (1), 831 (2000).

62. K. E. Sieh, "Prehistoric Large Earthquakes by Slip on the San Andreas Fault at Pallett Creek, California," J. Geophys. Res. **83** (B8), 3907−3939 (1978).

63. V. G. Trifonov, "The Map of Active Faults in Eurasia: Principles, Methods, and Results," J. Earthquake Prediction Res. **5** (3), 326−347 (1996).

64. V. G. Trifonov, "Using Active Faults for Estimating Seismic Hazard," J. Earthquake Predict. Res. **8** (2), 170−182 (2000).

65. V. G. Trifonov and M. N. Machette, "The World Map of Major Active Faults Project," Ann. Geofis. **36** (3−4), 225−236 (1993).

66. V. G. Trifonov, V. I. Makarov, and S. F. Skobelev, "The Talas-Fergana Active Right-Lateral Fault," Ann. Tectonicae Spec. Issue, Suppl. to Vol. 6, 224−237 (1992).

67. S. Z. Tutkun and S. B. Pavlides, "The Troy Fault," Bull. Geol. Soc. Greece **37**, 194–200 (2005).

68. R. E. Wallace, "Structure of a Portion of the San Andreas Rift in Southern California," Geo-Mar. Lett. **60** (4), 781–806 (1949).

69. R. E. Wallace, "Notes on Stream Channels Offset by the San Andreas Fault, Southern Coast Ranges, California," in *Proceedings of Conf. on Geol. Probl. of San Andreas Fault System* (Stanford Univ. Publ. Geol. Sci., 1968), Vol. 11, pp. 6–20.

70. D. L. Wells and K. H. Coppersmith, "Empirical Relationships among Magnitude, Rupture Length, Rupture Area, and Surface Displacement," Bull. Seismol. Soc. Amer. **84**, 974–1002 (1994).

71. D. M. Worral, V. Kruglyak, F. Kunst, and V. Kuznetsov, "Tertiary Tectonics of the Sea of Okhotsk, Russia: Far-Field Effects of the India–Eurasia Collision," Tectonics **15** (4), 813–826 (1996).

72. R. S. Yeats, K. Sieh, and C. R. Allen, *The Geology of Earthquakes* (Oxford Univ. Press, New York, 1997).